Original Article

Institution of MECHANICAL ENGINEERS
Journal of AUTOMOBILE ENGINEERING

Proc IMechE Part D:
J Automobile Engineering
2015, Vol. 229(3) 296–310

DOI: 10.1177/0954407014539674
pid.sagepub.com
SAGE

Virtual serial strategy for parallel hybrid electric vehicles

Alfonso Pantoja-Vazquez, Luis Alvarez-Icaza and Guillermo Becerra

Abstract

A new strategy to control the power split in hybrid electric vehicles is presented. The strategy is proposed for a parallel hybrid vehicle where the internal-combustion engine and the electric machine are coupled by a planetary gear system. This low computational burden strategy is designed to operate the internal-combustion engine at the maximum efficiency most of the time, in a similar fashion to serial hybrid electric vehicles, and to keep the state of charge of the battery on a desired level by an easy-to-tune proportional–integral controller. Although the strategy is not formally proven to be optimal, it is inspired by optimal control theory and has the advantage, when compared with optimal strategies, of requiring almost no a priori information about the vehicle or the route.

Keywords

Parallel hybrid vehicles, planetary gear system, fuel consumption efficiency, state of charge of the battery

Date received: 14 October 2013; accepted: 28 April 2014

Introduction

Global warming and shortage of fossil fuels, with all their socio-economical impacts, have made a reduction in energy consumption in human transportation an important goal for today's society. This reduction has been a challenge undertaken by governments, industry and researchers over the last few years.[1,2]

Hybrid electric vehicles (HEVs) are an option for helping to solve these problems. They use a combination of two or more power sources, usually an internal-combustion engine (ICE) and an electric machine (EM). HEVs can reduce fuel consumption and pollutant emissions, compared with conventional vehicles, owing to the extra degree of freedom added by the EM, which allows a more efficient use of the ICE and because of their ability to recover energy through regenerative braking. All these benefits should be available without sacrificing a vehicle's conventional attributes such as the performance, the safety and the reliability. The extent of the benefits depends on the fuel economy performance of HEVs which, in turn, is strongly related to the power-split strategy that decides at any time how much power must be delivered by each power source.[3–5]

HEVs may have different architectures that require the use of diverse energy management strategies. The main architectures, as presented by Millerin,[6] are series, parallel or series–parallel. A comparison of these was presented by Ehsani et al.,[7] together with their advantages and disadvantages.

In the literature, several design approaches have been proposed to control the power split on HEVs. Some of these are based on heuristics approaches, such as fuzzy logic,[2,8] fuzzy logic tuned with genetic algorithms[9] and rule-based strategies optimized with dynamic programming (DP).[3,10] Approaches based on optimal control theory were given, for example, by Delprat et al.[11,12] and Kessels et al.[13] The equivalent consumption minimization strategy (ECMS), an optimization strategy based on assuming an equivalence between the electric energy and the fuel energy, was presented by Sciaretta et al.[5] and Paganelli et al.[14] A proposal based on predictive control, a local optimization strategy, was described by Borhan et al.[15] There are also approaches based on DP or which use DP to tune a proposed strategy, such as those presented by Lin et al.,[3] Johannesson et al.[16] and van Keulen et al.[17]

Instituto de Ingeniería, Universidad Nacional Autónoma de México, Coyoacán, Distrito Federal 04510, México

Corresponding author:
Luis Alvarez-Icaza, Instituto de Ingeniería, Universidad Nacional Autónoma de México, Coyoacán, Distrito Federal 04510, México.
Email: alvar@pumas.iingen.unam.mx

A problem at the core of all power-split strategies for HEVs is the trade-off between the computational burden and the real-time implementation. On the one hand, optimization-based strategies have very high computational loads, which increase with increasing complexity of the vehicle models used for calculation. This prevents their real-time application and, therefore, calculations must be made offline using standard driving cycles as the basis for the computations. The changes in the driving conditions with respect to those used for the optimization are such that, in practice, optimality is lost. The optimal strategy that is most used in the literature is DP, the solution of which is not suitable for online implementation because of its dependence on the future driving conditions and owing to the high computational burden inherent in its solution construction.

On the other hand, strategies that are real time implementable are not optimal and must resort to simplified (static or dynamic) models of the HEV components. The two features that are most important to measure the success of a given non-optimal strategy are their overall performance in terms of fuel consumption when compared with normal non-HEVs and the ease of tuning.[9,18] The ECMS,[5,14] one of the most popular strategies, is easier to implement than optimal strategies; however, its performance may degrade if the driving conditions differ from those used to tune its parameters. An adaptive version of the ECMS was presented by Musardo et al.,[4] which partially alleviates this limitation. Rule-based strategies are mainly used for production vehicles, since they are easy to implement. However, for a given driving cycle, the performance is poor, compared with the DP solutions. The performance may depend on the driving cycle, and the state of charge (SOC) of the battery cannot be guaranteed.[18]

The approach undertaken in this paper is heuristic. The goal is to propose a strategy which requires little information, which can be implemented in real time and whose functioning is inspired by optimal strategies. However, the strategy proposed in this paper does not achieve the global minimum fuel consumption. It tries to close the gap between the performances of optimal strategies and the performances of heuristic strategies. This new strategy tries to recover the high-efficiency benefits of an HEV series configuration, by constraining the ICE to operate most efficiently, while keeping the advantages of an HEV parallel configuration. The strategy does not optimize the use of the EM, which has to accommodate its power and efficiency to the requirements of the driving cycle and the battery's SOC. This use of the EM does not normally have a great impact as the levels and sizes of the regions for high-efficiency operation of the EM are much larger than those of the ICE.

This paper extends the results of a strategy proposed by Becerra et al.[19] for parallel HEVs, which takes advantage of the kinematic and dynamic constraints of a planetary gear system (PGS) used as the mechanical coupling between the ICE and the EM. These constraints yield one more degree of freedom for the power split. Although the proposed strategy is not formally proven to be optimal, it is inspired by the cost functions of some optimal problems that propose a trade-off between maintaining the SOC of the batteries and using as little fuel as possible.

The strategy presented in this work has the advantages of being easy to implement in real time and having low computational requirements when compared with optimal strategies. The ICE performance is represented by a curve that is obtained offline with a static map available from the ADVISOR database.[20] The extra degree of freedom provided by the PGS which couples the ICE and the EM is used to keep the ICE operating in its most efficient conditions almost all the time. The EM delivers or receives the lack or excess of power required by the driving cycle. Regulation of the battery's SOC to a reference value is achieved by means of a proportional–integral (PI) controller, which guarantees smooth changes in the operation of the power-split strategy. Regenerative braking is also accommodated by the strategy in a natural fashion, although in this case the efficiency of the EM cannot be optimized, as the power to absorb must satisfy the driving cycle constraints.

The rest of this paper is organized as follows. In the second section, the configuration and the models used for simulations of the HEV are presented; in the third section, the problem of the power split is formulated and the *virtual serial strategy* is presented; simulation results of the proposed strategy over several driving cycles and its parameter robustness are analysed in the fourth section; finally, conclusions and future work are presented in the fifth section.

Parallel hybrid vehicle model

The HEV configuration selected in this work is a parallel configuration, where the ICE and the EM are coupled via a PGS (Figure 1), as proposed by Becerra et al.[19]

Vehicle model

The power P_p requested by the power train is calculated by modelling the vehicle as a moving mass subject to a traction force F_{tr} provided by the two power sources.[3] The velocity dynamics $v(t)$ of the vehicle are given by

$$m\frac{\mathrm{d}v(t)}{\mathrm{d}t} = F_{tr} - \frac{1}{2}\rho_a C_d A_d [v(t)]^2 - mgC_r \cos[\gamma(t)] - mg\sin[\gamma(t)] \quad (1)$$

where ρ_a is the density of air, C_d is the aerodynamic drag coefficient, A_d is the frontal area of the vehicle, m is the mass of the vehicle including the mass of the cargo, g is the acceleration due to gravity, C_r is the rolling resistance coefficient of the tyre and $\gamma(t)$ is the slope of the road.

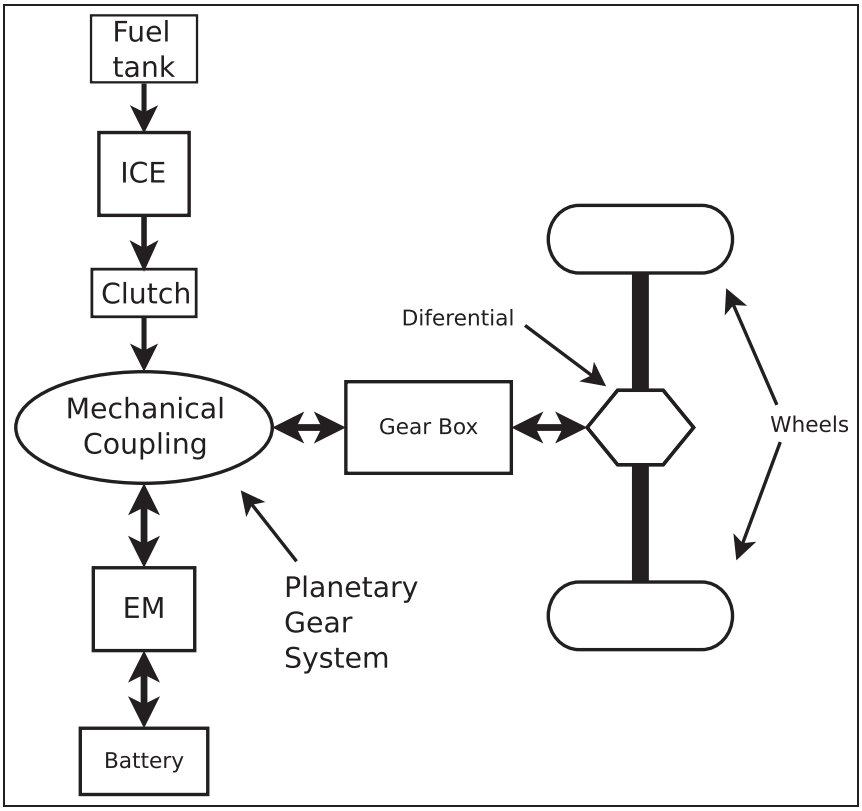

Figure 1. Parallel HEV configuration.
ICE: internal-combustion engine; EM: electric machine.

The torque τ_p and speed ω_p demanded by the powertrain are

$$\omega_p = \frac{R_f}{R_w} R(t) v(t) \tag{2}$$

and

$$\tau_p = \frac{R_w}{R_f} \frac{1}{R(t)} F_{tr} \tag{3}$$

respectively, where $R(t)$ is the gearbox ratio, R_f is the final drive ratio and R_w is the radius of the wheels.

Finally, the power required at the output of the powertrain is

$$\begin{aligned} P_p(t) &= \omega_p(t)\tau_p(t) \\ &= v(t)F_{tr}(t) + P_{acc} \end{aligned} \tag{4}$$

where P_{acc} is the power required by the vehicle accessories. The sum of the required power $v(t)F_{tr}(t)$ to accelerate the vehicle and the powerP_{acc} demanded by the vehicle accessories yields the power $\omega_p(t)\tau_p(t)$ that the powertrain must provide.

Internal-combustion engine model

The ICE is modelled through a static non-linear map, taken from ADVISOR,[20] which relates the fuel rate consumption $\dot{m}_f$ of the ICE to the torque τ_{ice} at the crankshaft and the engine speed ω_{ice}or, in other words,

$$\dot{m}_f = f(\omega_{ice}, \tau_{ice}) \tag{5}$$

Using the lower heating value of the fuel, the ICE efficiency map can be generated. Figure 2 shows the map for the ICE used in this work. From the efficiency point of view, it is desirable to operate the ICE on the most efficient points of this map.

Electric machine model

In an HEV, the EM can function as a motor or a generator depending on whether it is required to give or receive power. The EM is modelled also by a static non-linear map which relates the EM speed ω_{em} and the EM torque τ_{em} to the efficiency η_{gen} when the EM works as a generator, and another map which relates the EM speed ω_{em} and the EM torque τ_{em} to the efficiency η_{mot} when the EM works as a motor.

In other words, if the EM works as a motor ($\tau_{em} \geqslant 0$), then

$$P_{em} = \eta_{mot}(\tau_{em}, \omega_{em}) P_{bat} \tag{6}$$

or, if it works as a generator ($\tau_{em} < 0$), then the electric power P_{bat} is given by

$$P_{bat} = \eta_{gen}(\tau_{em}, \omega_{em}) P_{em} \tag{7}$$

with $P_{em} = \tau_{em}\omega_{em}$.

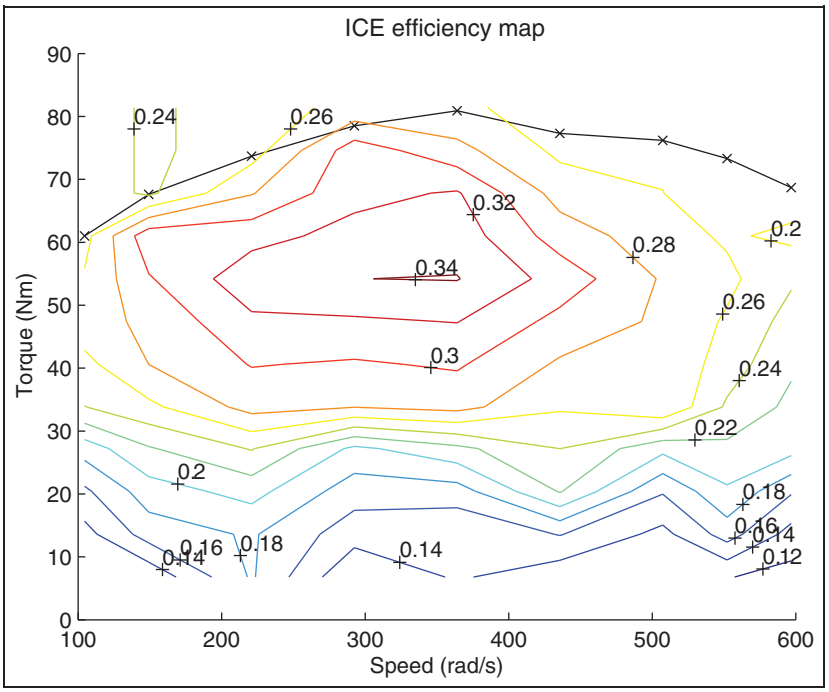

Figure 2. The ICE efficiency map.
ICE: internal-combustion engine.

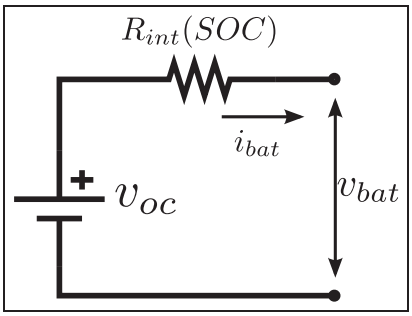

Figure 3. The equivalent circuit of the battery.
SOC: state of charge.

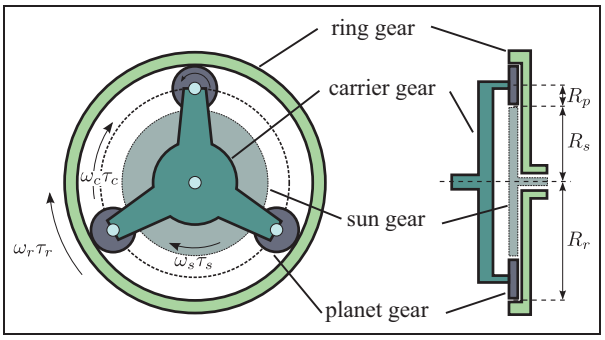

Figure 4. The PGS.

Battery

The battery is modelled as a voltage source v_{oc} with an internal resistance R_{int} which depends on the SOC.[3] The equivalent circuit is shown in Figure 3, where v_{oc} is the battery's open-circuit voltage, i_{bat} is the bus current and v_{bat} is the bus voltage.

Using the Kirchoff voltage law, i_{bat} is found by solving

$$R_{int}(\text{SOC})i_{bat}^2 - v_{oc}i_{bat} + P_{bat} = 0 \tag{8}$$

and v_{bat} is given by

$$v_{bat} = v_{oc} - R_{int}(\text{SOC})i_{bat} \tag{9}$$

Finally, the SOC is obtained from the expression

$$\text{SOC}(t) = \min\left\{1, \max\left[0, Q_0 - \frac{\int_{t_0}^{t} i_{bat}(\tau)\,\mathrm{d}\tau}{Q_T}\right]\right\} \tag{10}$$

where Q_0 is the initial charge and Q_T is the total charge that the battery can store.

Planetary gear system

A PGS is used as the mechanical coupling between the ICE and the EM, as proposed by Becerra et al.[19] A schematic diagram is shown in Figure 4. With this coupling, the ICE output shaft is connected to the sun gear, the EM is connected to the ring gear and the gearbox is connected to the carrier shaft.

Defining $k = R_r/R_s$, with R_r the radius of the ring gear and R_s the radius of the sun gear, the angular speeds on the PGS satisfy

$$\omega_c = \frac{1}{k+1}\omega_s + \frac{k}{k+1}\omega_r \tag{11}$$

and the balance of power is given by

$$\tau_c \omega_c = \tau_s \omega_s + \tau_r \omega_r \quad (12)$$

where ω is the angular speed, τ is the torque and the subscripts s, c and r refer to the sun gear, the planet carrier and the ring gear respectively.

Virtual serial strategy

The problem to be solved, from the optimization point of view, is to minimize the fuel consumption over a desired driving cycle according to

$$\min J = \int_0^{t_c} \dot{m}_f \left(\omega_{ice}(t), \tau_{ice}(t)\right) dt \quad (13)$$

subject to

$$\omega_{ice\ min} \leqslant \omega_{ice}(t) \leqslant \omega_{ice\ max} \quad (14)$$
$$\tau_{ice\ min} \leqslant \tau_{ice}(t) \leqslant \tau_{ice\ max} \quad (15)$$
$$\omega_{em\ min} \leqslant \omega_{em}(t) \leqslant \omega_{em\ max} \quad (16)$$
$$\tau_{em\ min} \leqslant \tau_{em}(t) \leqslant \tau_{em\ max} \quad (17)$$
$$P_{bat\ min} \leqslant P_{bat} \leqslant P_{bat\ max} \quad (18)$$
$$\mathrm{SOC}_{min} \leqslant \mathrm{SOC}(t) \leqslant \mathrm{SOC}_{max} \quad (19)$$

Rewriting equations (11) and (12) in terms of the ICE and EM variables, the two equations that constrain the demanded power are

$$\begin{aligned} P_p(t) &= \tau_p(t)\omega_p(t) \\ &= \tau_{ice}(t)\omega_{ice}(t) + \tau_{em}(t)\omega_{em}(t) \\ &= P_{em}(t) + P_{ice}(t) \end{aligned} \quad (20)$$

and

$$\omega_p(t) = \frac{1}{k+1}\omega_{ice}(t) + \frac{k}{k+1}\omega_{em}(t) \quad (21)$$

where the subscript *ice* is associated with the sun gear, the subscript *em* with the ring gear and the subscript *p* with the final drive coupled to the carrier gear. The subscripts *min* and *max* mean the minimum value and the maximum value respectively for the constrained variable and t_c is the duration of the driving cycle.

When the ICE is used, a feasible solution to the power-split problem would be to operate it in only the regions where it spends less fuel per power generated, i.e. at the most efficient operation points. Considering this, the problem stated in equation (13) can be rewritten as

$$\max J = \int_0^{t_c} \mathrm{ICE}_{eff} \left(\omega_{ice}(t), \tau_{ice}(t)\right) \mathrm{d}t \quad (22)$$

subject to the same constraints as the problem from equation (13) and where ICE_{eff} is the ICE efficiency. The strategy proposed in this work is based on this consideration, and it is called the virtual serial strategy because, in a serial HEV configuration, the ICE is always operated at it most efficient points.

In addition to keeping the ICE in its most efficient region when it is used, the vehicle must follow the driving cycle. In consequence, the problem to be solved is to meet the power P_p on the output of the PGS, while the ICE operates in its most efficient region. This problem of providing the power P_p has multiple solutions, since many combinations of the torque and the speed at each power source can yield the demanded power P_p.

The approach presented in this work is based on the following assumptions.

1. The strategy meets the required power to perform the driving cycle, if it is feasible.
2. The ICE operation is optimized in order to operate the ICE at its highest efficient power, when possible.
3. Once the ICE power has been set, the EM is used to generate or absorb the lack or excess of required power.
4. A PI controller adjusts dynamically the use of the ICE in order to keep the SOC near a given reference value SOC_{ref}.

A block diagram of the proposed strategy is shown in Figure 5 and will be detailed in the following sections.

Power of the internal-combustion engine

When $P_p > 0$, the first step of this strategy is to determine a pre-value for the ICE power $\hat{P}_{ice}$. The final value P_{ice} could change later, if necessary to guarantee tracking of the driving cycle. In most cases, however, $\hat{P}_{ice}$ will be the final ICE power.

There are two cases when the ICE should operate away from its maximum efficiency operation point $\mathrm{ICE}_{eff\ max}$, and they are as follows.

1. When the required driving cycle power is very low or very high, the ICE should be off or should complement the lack of power respectively.
2. When the SOC is not at its given reference value, the ICE must try to charge the batteries by giving more power than that required for propulsion if the SOC is below its reference value, or to

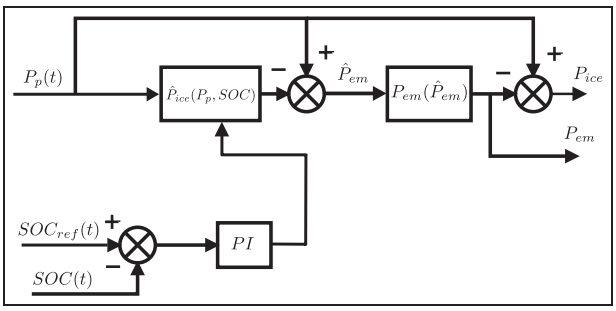

Figure 5. The power-split strategy diagram.
SOC: state of charge.

discharge the batteries by giving less power than that required for propulsion if the SOC is above its reference value.

A bang–bang type of solution[21] would be to saturate the ICE power when the previous cases occur, but instead, as in the work by Becerra et al.,[19] a soft curve is proposed on the basis of the previous observations. This means, for example, that, when the SOC is below the reference value, instead of giving all the available ICE power $P_{ice\ max}$, the extra power given by the ICE will be limited by a soft curve. In consequence, this curve depends on the required power and on the SOC according to

$$\hat{P}_{ice}(\hat{P}_p(t), \mathrm{SOC}(t)) = \alpha(\hat{P}_p(t), \mathrm{SOC}(t)) P_{ice\ max} \tag{23}$$

where $\hat{P}_p(t)$ is the normalized value of $P_p(t)$ defined as $\hat{P}_p(t) = P_p(t)/P_{ice\ max}$ and $\alpha(\hat{P}_p(t), \mathrm{SOC}(t))$ is designed to make the ICE work at its most efficient power as much as possible. This means that $\alpha(\hat{P}_p(t), \mathrm{SOC}(t))$ should remain at $P_{ice\_eff}/P_{ice\ max}$ for a wide range of $\hat{P}_p(t)$, where P_{ice_eff} is the most efficient power of the ICE. When the SOC is at its desired value, i.e. $\mathrm{SOC}(t) = \mathrm{SOC}_{ref}$, the shape of $\alpha(\hat{P}_p(t), \mathrm{SOC}(t))$ versus $\hat{P}_p(t)$ should be like the plot in Figure 6.

The structure proposed here to generate the function $\alpha(\hat{P}_p(t), \mathrm{SOC}(t))$ is a seventh-order polynomial of the form

$$\alpha(\hat{P}_p(t), \mathrm{SOC}(t)) = \left\{ \left[2\hat{P}_p(t) - 1 + \xi + \mathrm{SOC}_{comp}(\mathrm{SOC}(t)) \right]^7 + \mu \right\} \gamma \tag{24}$$

where the parameters ξ, μ, γ and SOC_{comp} (a value produced by a PI compensator) are described later. The design of $\alpha(\hat{P}_p(t), \mathrm{SOC}(t))$ was focused on an increasing value function, which is symmetric and has a wide flat portion over most of its range. A seventh-order polynomial was chosen because its calculation is easy. Different choices, such as a hyperbolic tangent, could also be used as long they have a similar shape. The function $\alpha(\hat{P}_p(t), \mathrm{SOC}(t))$ ranges between 0 and 1, and the rationale behind its design is described below.

Considering $\mathrm{SOC}_{comp} = 0$, which corresponds to $\mathrm{SOC}(t) = \mathrm{SOC}_{ref}$, the parameters ξ, μ and γ must satisfy the conditions

$$\alpha(\hat{P}_p(t), \mathrm{SOC}_{ref})|_{\hat{P}_p = 0} = 0 \tag{25}$$

$$\alpha(\hat{P}_p(t), \mathrm{SOC}_{ref})|_{\hat{P}_p = 1} = 1 \tag{26}$$

and, for a certain $\hat{P}_0 \in [0, 1]$,

$$\alpha(\hat{P}_p(t), \mathrm{SOC}_{ref})|_{\hat{P}_p = \hat{P}_0} = \frac{P_{ice\_eff}}{P_{ice\ max}} \tag{27}$$

$$\left. \frac{\partial \alpha}{\partial \hat{P}_p} \right|_{\hat{P}_p = \hat{P}_0} = 0 \tag{28}$$

Solving equations (25) to (28) for ξ, μ and γ yields

$$\xi = \frac{\sqrt[7]{P_{ice\ max}/P_{ice\_eff} - 1} - 1}{\sqrt[7]{P_{ice\ max}/P_{ice\_eff} - 1} + 1} \tag{29}$$

$$\gamma = \frac{1 - P_{ice\_eff}/P_{ice\ max}}{(1 + \xi)^7} \tag{30}$$

$$\mu = \frac{P_{ice\_eff}}{\gamma P_{ice\ max}} \tag{31}$$

and $\hat{P}_0 = (1 - \xi)/2$.

Figure 7 shows $\alpha(\hat{P}_p(t), \mathrm{SOC}_{ref})$ for $P_{ice\_eff}/P_{ice\ max} = 0.5$, which corresponds to the efficiency map from Figure 2 with $\mathrm{SOC}_{comp} = 0$.

The role of $\mathrm{SOC}_{comp} \in [-1, 1]$ is to move the power calculated in equation (24) at time t according to the

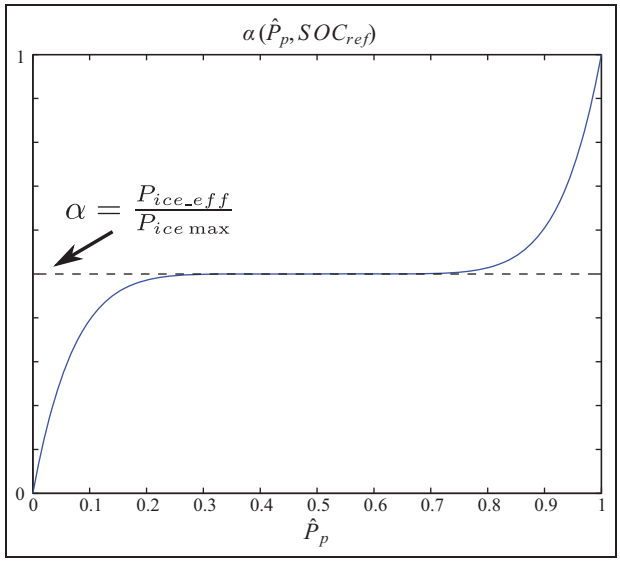

Figure 6. Plot of $\alpha(\hat{P}_p(t), \mathrm{SOC}_{ref}(t))$.
SOC: state of charge.

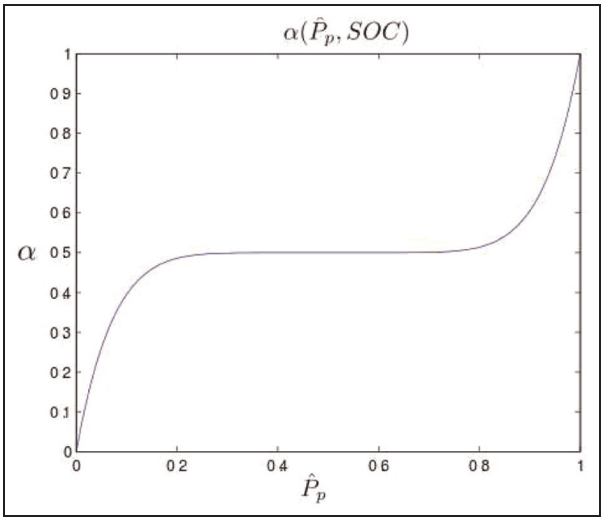

Figure 7. Plot of $\alpha(\hat{P}_p(t), \mathrm{SOC}(t))$.
SOC: state of charge.

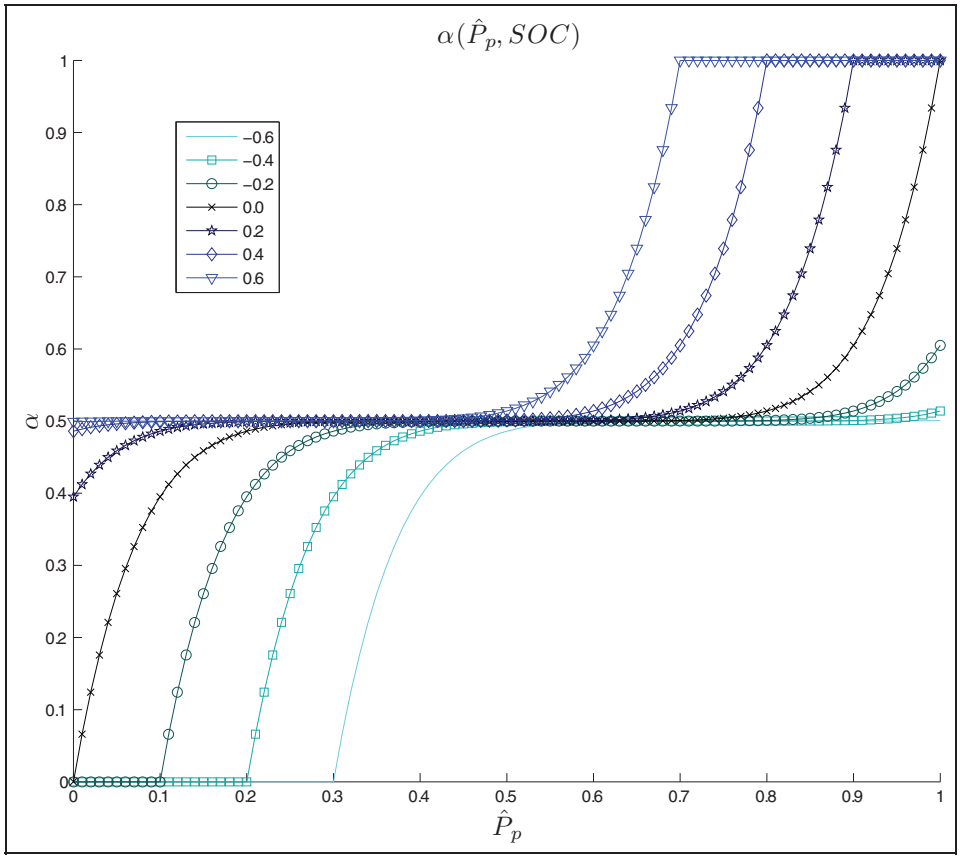

Figure 8. Plot of $\alpha(\hat{P}_p(t), \mathrm{SOC}(t))$ for several values of SOC_{comp}.
SOC: state of charge.

difference between $\mathrm{SOC}(t)$ and its reference value SOC_{ref}. In other words, if $\mathrm{SOC}(t)$ is below SOC_{ref}, more use of the ICE is expected to recharge the batteries and, if $\mathrm{SOC}(t)$ is above SOC_{ref}, less use of the ICE is expected, as there is an excess of energy in the batteries.

Figure 8 shows the plot of $\alpha(\hat{P}_p(t), \mathrm{SOC}(t))$ for several values of SOC_{comp}. It can be seen that, to bring $\mathrm{SOC}(t)$ to the desired SOC_{ref} value, positive values of SOC_{comp} are expected when $\mathrm{SOC}(t)$ is below SOC_{ref}, and negative values of SOC_{comp} are expected when $\mathrm{SOC}(t)$ is above SOC_{ref}.

To keep the value of $\mathrm{SOC}(t)$ at its desired reference value SOC_{ref}, the calculation of SOC_{comp} is based on a PI controller. This controller is necessary because, without it, $\alpha(\hat{P}_p(t), \mathrm{SOC}(t))$ tends to fill up or to deplete the battery, depending on the driving cycle. SOC_{comp} is defined as

$$\mathrm{SOC}_{comp}(\mathrm{SOC}(t)) = k_p\left[\mathrm{SOC}_{ref} - \mathrm{SOC}(t)\right] + k_i \int_0^t \left[\mathrm{SOC}_{ref} - \mathrm{SOC}(\tau)\right] \mathrm{d}\tau$$

where k_i and k_p are the tuning parameters of the PI controller. The value of SOC_{comp} is saturated to guarantee that $\mathrm{SOC}_{comp} \in [-1, 1]$.

At this point, a first proposal for the ICE power $\hat{P}_{ice}(t)$ is calculated on the basis of equation (23). The final $P_{ice}(t)$ is set after the EM power is determined, to assure meeting the requested power, as illustrated in Figure 5. Setting of the EM power is explained later. The final value for P_{ice} is

$$P_{ice}(t) = \max\left[\hat{P}_{ice}(t), P_p(t) - P_{em}(t)\right] \tag{32}$$

which is saturated between 0 and $P_{ice\,max}$. Note, from Figure 8, that the curve $\alpha(\hat{P}_p(t), \mathrm{SOC}(t))$ has abrupt transitions in 0 and $P_{ice\,max}$. To avoid these, a low-pass filter is applied with a critical frequency of 1.25 Hz, which eliminates the sudden changes in the required power P_{ice} and helps to reduce the acceleration spikes.

Once P_{ice} has been set, ω_{ice} and τ_{ice} need to be determined. Taking advantage of the kinematic relation of the PGS expressed in equation (20), ω_{ice} can be set to obtain the maximum efficiency for the ICE at a given power. This is achieved with the help of the curve shown in Figure 9, which, for a given P_{ice}, yields the value of ω_{ice} where the ICE operates most efficiently and where the calculation is based on the algorithm presented in Appendix 1. Finally, the ICE torque is set with

$$\tau_{ice}(t) = \begin{cases} 0 & \text{for } \omega_{ice}(t) = 0 \\ \frac{P_{ice}(t)}{\omega_{ice}(t)} & \text{for } \omega_{ice}(t) > 0 \end{cases} \tag{33}$$

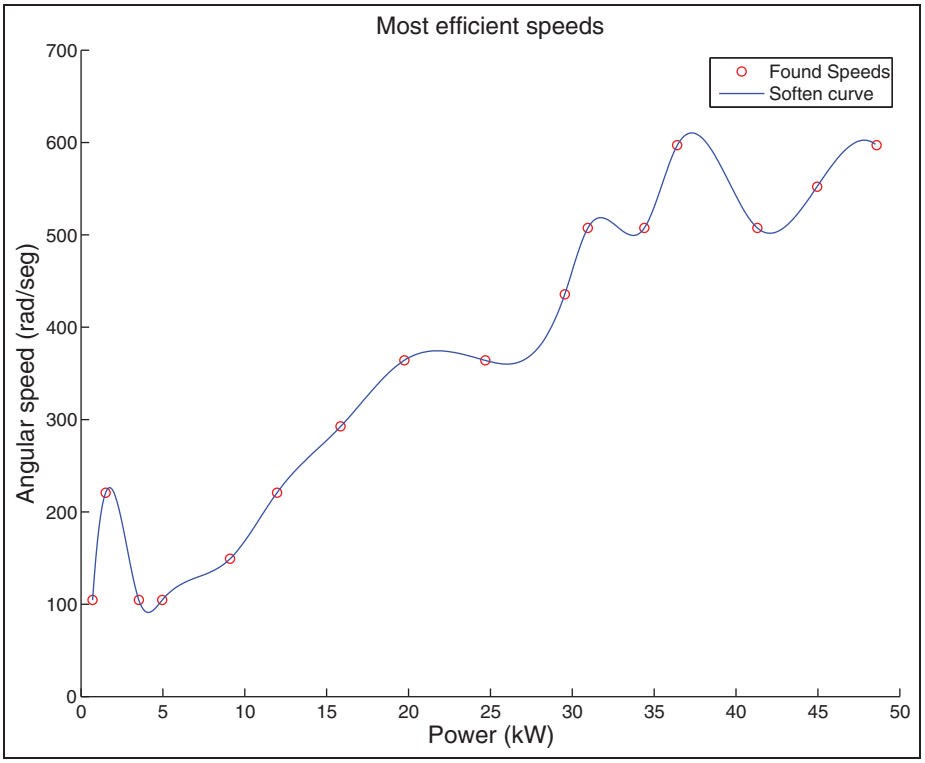

Figure 9. ICE power versus efficient speed.

Power of the electric machine

It is expected that the EM compensates the difference between P_p and P_{ice} in order to meet the required power, although it is limited by the maximum power $P_{em\,max}$ of the EM and the minimum power $P_{em\,min}$ of the EM. As shown in Figure 5, a pre-value for the EM power is

$$\hat{P}_{em}(t) = P_p(t) - \hat{P}_{ice}(t) \tag{34}$$

and the final value for the EM power is

$$P_{em}(\hat{P}_{em}(t)) = \max\{P_{em\,min}, \min[P_{em\,max}, \hat{P}_{em}(t)]\} \tag{35}$$

Finally, from equation (20), the EM speed and torque are calculated as

$$\omega_{em}(t) = \frac{k+1}{k}\left[\omega_p(t) - \frac{\omega_{ice}}{k+1}(t)\right] \tag{36}$$

and

$$\tau_{em}(t) = \begin{cases} 0 & \text{for } \omega_{em}(t) = 0 \\ \frac{P_{em}(t)}{\omega_{em}(t)} & \text{for } \omega_{em}(t) \neq 0 \end{cases} \tag{37}$$

respectively.

Regenerative braking

In the case of braking ($P_p(t) < 0$), it is necessary to recover as much energy as possible, taking care not to damage the batteries.[19] In this case, $P_{ice}(t) = 0$ and $P_{em}(t)$ is given by

$$P_{em}(\mathrm{SOC}(t)) = \max[P_p(t),\ \beta(\mathrm{SOC}(t))P_{em\,max}] \tag{38}$$

with

$$\beta(\mathrm{SOC}(t)) = 0.5(\tanh\{A_1[\mathrm{SOC}(t) - \mathrm{SOC}_{max}]\}) - 0.5 \tag{39}$$

where A_1 is a design parameter. Figure 10 shows the plot of β for $A_1 = 0.8$ and $\mathrm{SOC}_{max} = 90\%$.

Finally, the required power at the friction brakes is

$$P_f(t) = P_p(t) - P_{em}(t) \tag{40}$$

Note that optimization of the EM during regenerative braking cannot be attained, as in this case the EM is the only power source and the driving cycle demands must be met.

Simulation results

In this section, the results of simulations on the vehicle and the strategy presented in the previous sections using ADVISOR[20,22] are shown. ADVISOR was used as a simulation platform as it makes it possible to reproduce the results easily. To obtain an idea of the strategy performance, it is compared with a rule-based strategy,[23] available in ADVISOR as the default strategy, with the same vehicle parameters, with a normal parallel configuration and with the ICE and the EM connected through a gear with a different ratio for each. (More details have been given[24] about this rule-based strategy and can be consulted by interested

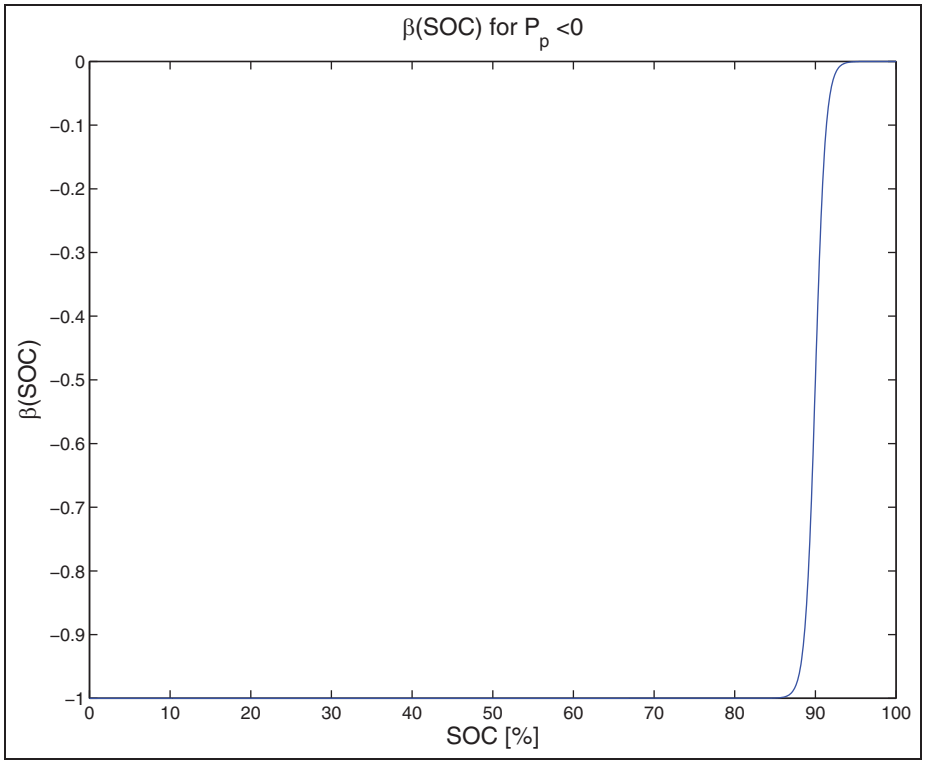

Figure 10. The regenerative braking power as a function of the SOC.
SOC: state of charge.

Table 1. Main parameters for the simulated vehicle.

Total mass	912 kg
Peak power of the internal-combustion engine	41 kW
Peak power of the lithium-ion battery (6 A h; V_{nom} = 267 V)	25 kW
Peak power of the electric machine	25 kW
Gearbox	Five speeds

Table 2. Power-split strategy parameters.

SOC_{ref}	70%
SOC_{max}	85%
A	1
k (PGS ratio)	5
P_{ice_eff}	20 kW
$P_{ice\ max}$	41 kW
k_p	1
k_i	0.01

SOC: state of charge; PGS: planetary gear system.

readers.) The main parameters for the simulated vehicle are shown in Table 1.

The strategy parameters are shown in Table 2. The ICE map was taken from the ADVISOR database.

The simulation results for the virtual serial strategy are shown in Figures 11 and 12, and the results for the rule-based strategy are shown in Figures 13 and 14. In the simulations of the new strategy the same tuning parameters were used for both driving cycles. This shows the robustness of the strategy, contrary to EMCS-based strategies that must be manually or adaptively tuned for each cycle.[4] The simulation results for the strategies are summarized in Table 3 which shows the fuel consumption values for both strategies and driving cycles.

Note that, from Figures 11 to 14, even though in terms of the velocity the driving cycles are apparently smooth signals, the power demanded in both driving cycles has abrupt changes, as indicated by the corresponding plots. It is clear that the virtual serial strategy eliminates most of these spikes on the demanded power in the ICE and that the power peaks are absorbed by the EM.

It is convenient to emphasize that the initial SOCs in the simulations were set, after several trials, to coincide with the final SOCs. Taking this into consideration, the fuel consumption is only due to the power-split strategy used to move the vehicle; it is not affected by the electrical energy in the storage system and gives a clear picture about the strategy performance. It is evident that there is a great improvement with the proposed strategy, especially for urban driving.

As can be appreciated in Figures 11 and 12, the ICE works mostly around its most efficient power, 19.7 kW. This is confirmed with the help of Figure 15 and Figure 16, which show the ICE efficiency histograms ($P_{ice} > 0$) for the UDDS cycle and the HWFET cycle respectively. It can be seen that the ICE functions at the maximum

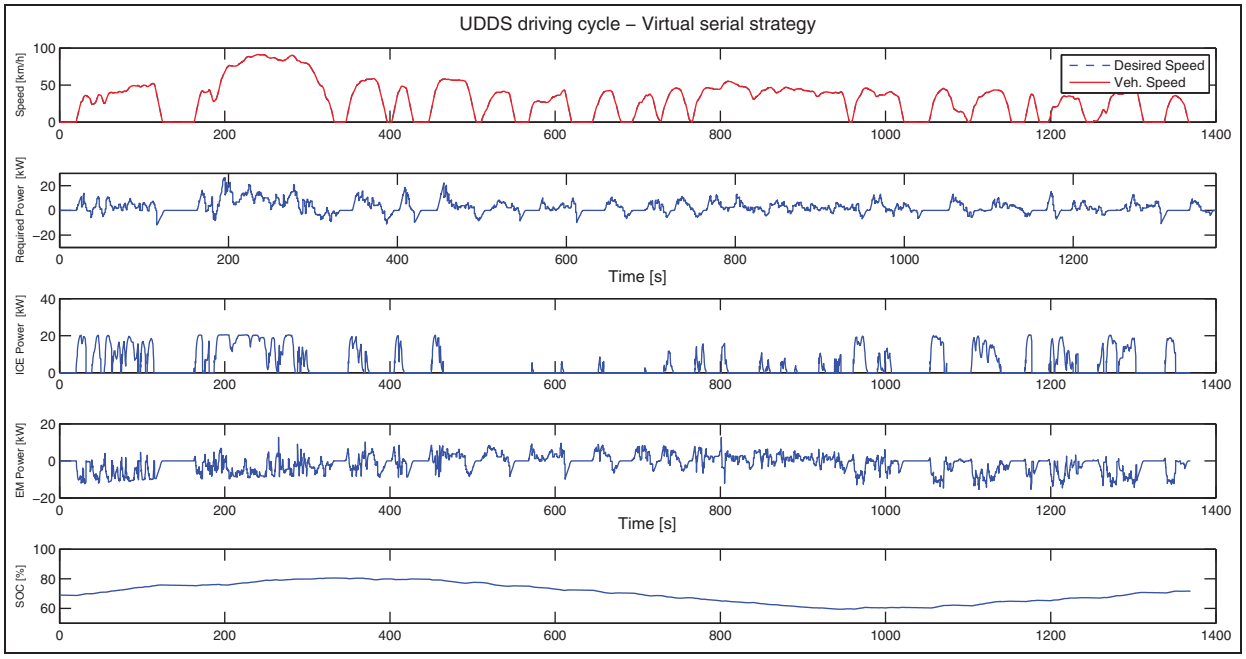

Figure 11. Virtual serial strategy on the UDDS cycle simulation results.
UDDS: Urban Dynamometer Driving Schedule; Veh.: vehicle; ICE: internal-combustion engine; EM: electric machine; SOC: state of charge.

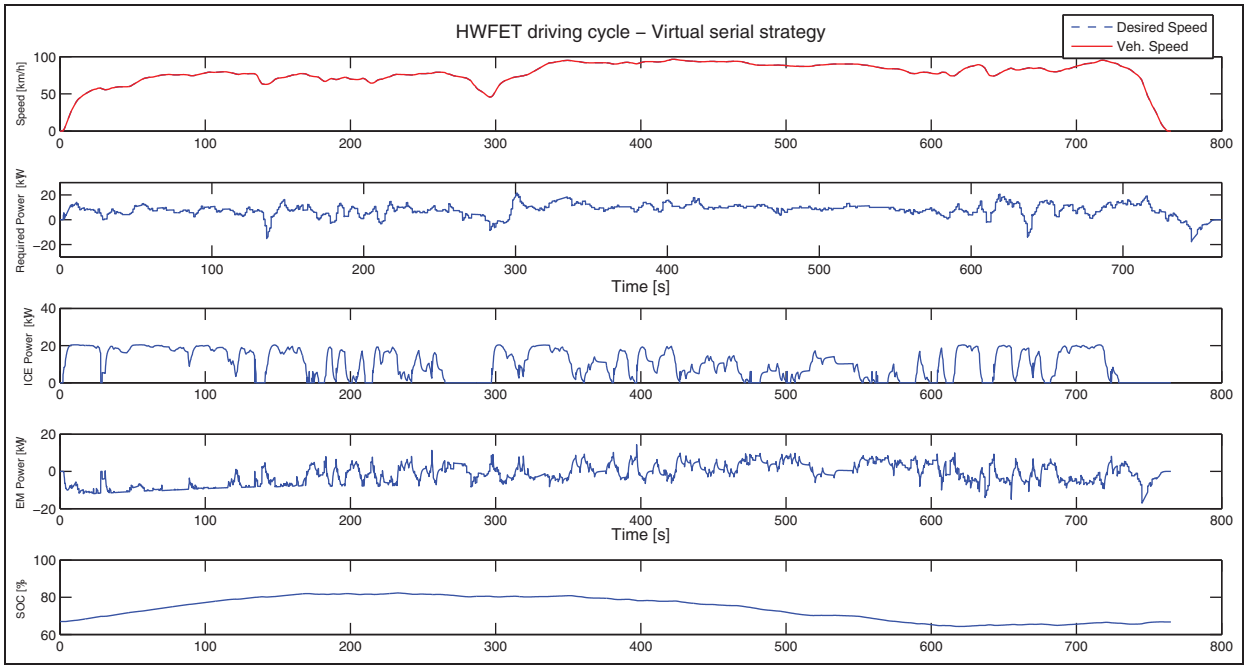

Figure 12. Virtual serial strategy on the HWFET cycle simulation results.
HWFET: Highway Fuel Economy Test; Veh.: vehicle; ICE: internal-combustion engine; EM: electric machine; SOC: state of charge.

efficiency about 50% of the time and that the very-low-efficiency points of operation are virtually eliminated. This has a clear impact on reducing the fuel consumption and, most importantly, the pollutant emissions.

Conclusions

In this work a new strategy for HEV power flow control was proposed, which is based on an innovative way to couple the power sources introduced by Becerra et al.[19] The new strategy resembles hybrid serial architectures, where the ICE operates at the maximum efficiency at all times. Although it is not proven to be optimal in terms of the fuel consumption, the strategy is inspired by the optimal control theory. As it requires little information and has low computational requirements, compared with other optimal power-split strategies, it is suitable for real-time implementation.

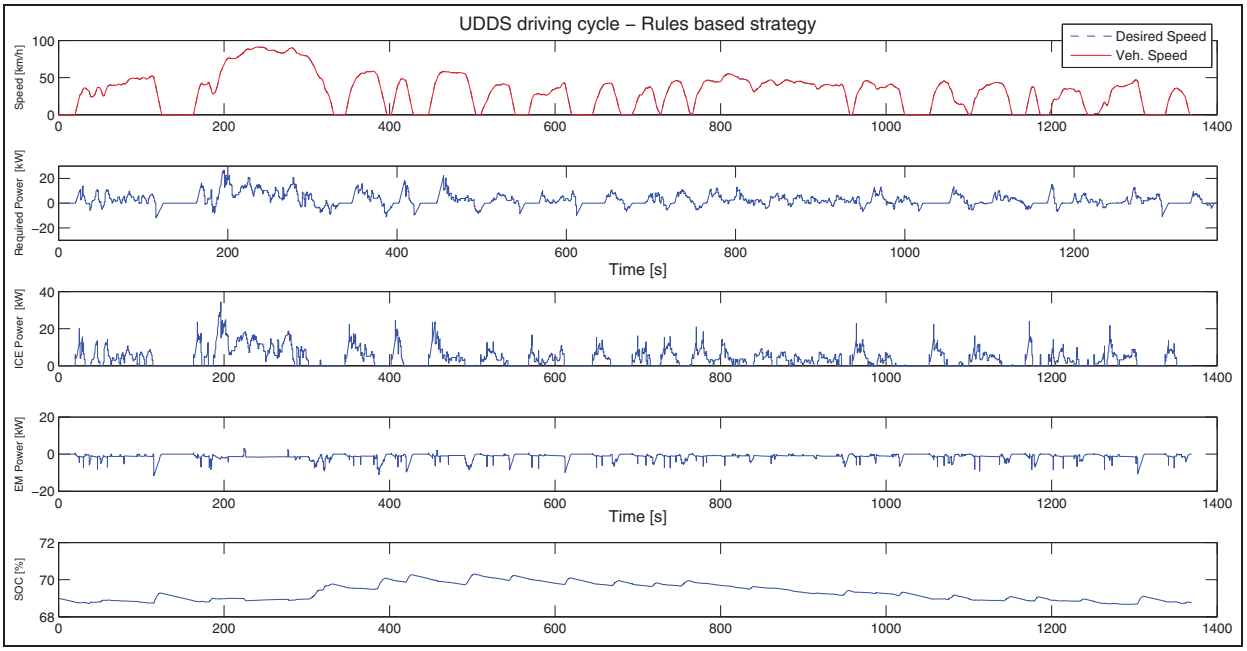

Figure 13. Rule-based strategy on the UDDS cycle simulation results.
UDDS: Urban Dynamometer Driving Schedule; Veh.: vehicle; ICE: internal-combustion engine; EM: electric machine; SOC: state of charge.

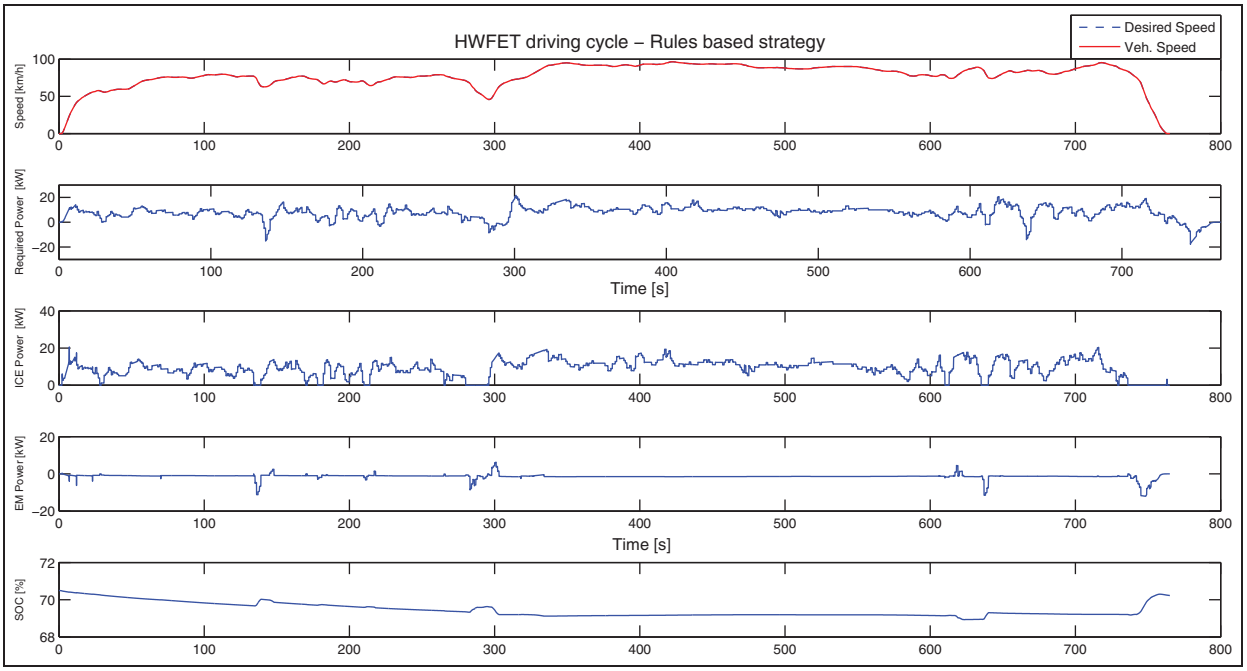

Figure 14. Rule-based strategy on the HWFET cycle simulation results.
HWFET: Highway Fuel Economy Test; Veh.: vehicle; ICE: internal-combustion engine; EM: electric machine; SOC: state of charge.

Table 3. Fuel consumption in the simulations.

Cycle	Strategy	Initial SOC (%)	Final SOC (%)	Fuel consumption (l/100 km)
UDDS	Virtual	71.14	71.14	5.31
UDDS	Rules	69.66	69.66	6.12
HWFET	Virtual	70.72	70.72	4.32
HWFET	Rules	71.5	71.5	4.75

SOC: state of charge; UDDS: Urban Dynamometer Driving Schedule; HWFET: Highway Fuel Economy Test.

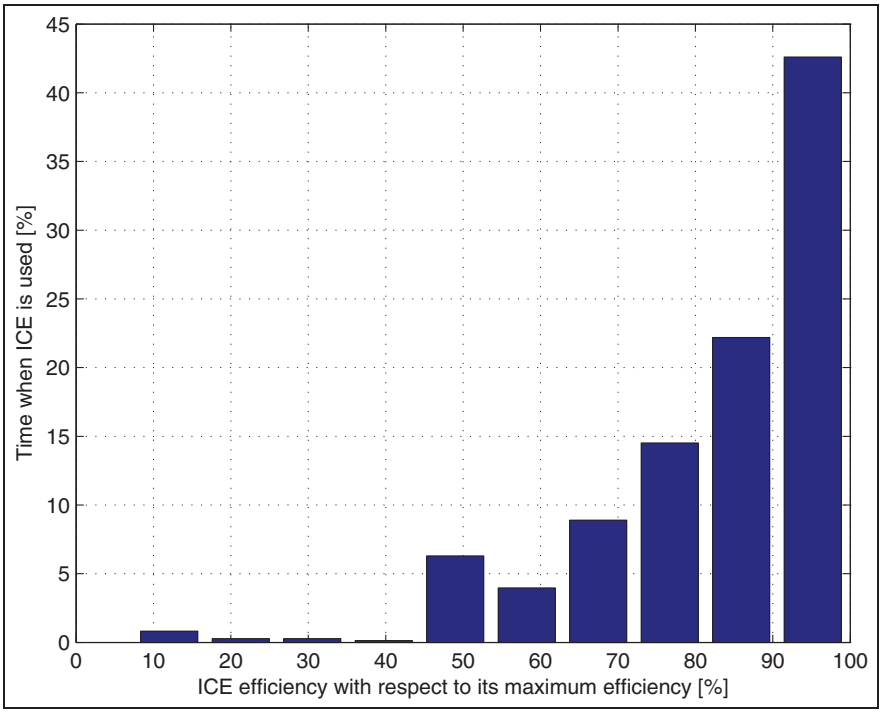

Figure 15. ICE efficiency histogram when the ICE is used in the UDDS cycle.
ICE: internal-combustion engine.

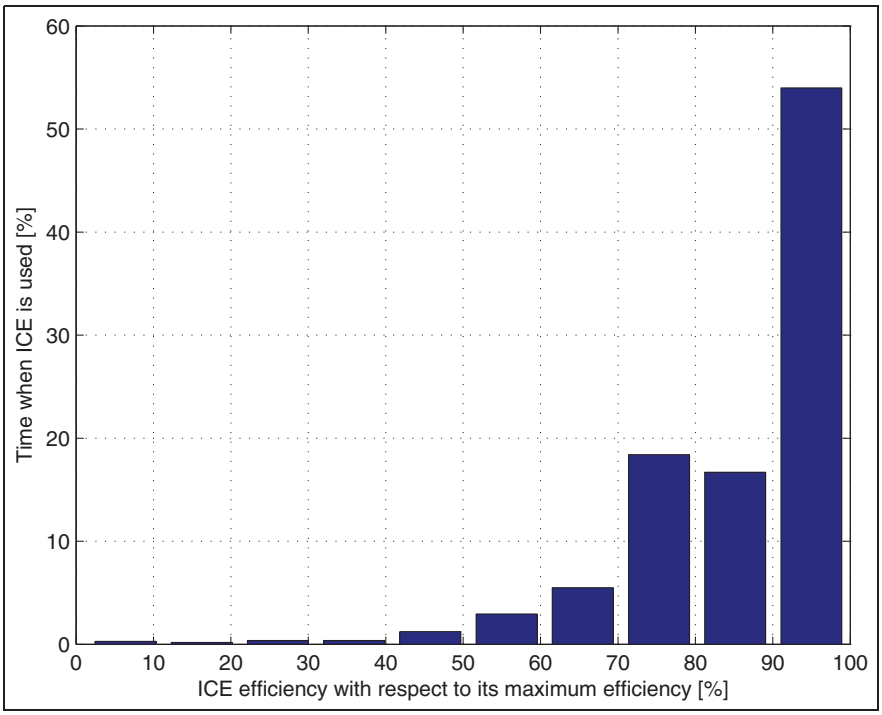

Figure 16. ICE efficiency histogram when the ICE is used in the HWFET cycle.
ICE: internal-combustion engine.

The strategy attains operation of the ICE in its most efficient region most of the time, similar to what happens in serial configuration HEVs. A PI controller was designed to compensate the deviation of the SOC from the desired reference value. This compensator provides a smooth power split and is easy to tune since since it depends on only two parameters. Although in this work a PI controller was used, other types of controller could be employed.

The virtual serial strategy exploits the fact that, in a modern injection-based ICE, combustion is very efficient. In this way, when this new strategy is used in

combination with normal fuel injection control techniques, the overall result is very positive. One the one hand, the virtual strategy reduces global fuel consumption while, on the other hand, the fuel injection control techniques optimize the pollutant emissions during acceleration. Therefore, the combination of the two techniques is complementary and helps to reduce the total emissions.

The steps to implement the strategy can be summarized as follows.

- Offline

1. Using the algorithm shown in Appendix 1, calculate the function that relates the required ICE power to the most efficient speed. This step is carried out only once. If no efficiency maps are available, the curve can be calculated by direct measurements.

- Online (if $P_p > 0$; otherwise the section on regenerative braking is used)

1. With the demanded power $P_p(t)$ and the SOC, calculate a pre-value of the ICE power, as shown in section on the ICE power.
2. With the demanded power $P_p(t)$ and the pre-value of the ICE power, calculate the EM power $P_{em}(t)$ in order to meet equation (21).
3. Using the EM power $P_{em}(t)$, calculate the ICE power $P_{ice}(t)$ to assure that the demanded power $P_p(t)$ is met, in case the EM power achieves its maximum power.
4. With the ICE power $P_{ice}(t)$ as the input, for the function calculated on the offline step, calculate the most efficient ICE speed $\omega_{ice}(t)$ for that given power.
5. Using equation (20), the demanded speed $\omega_p(t)$ and the ICE speed $\omega_{ice}(t)$, calculate the EM speed $\omega_{em}(t)$.
6. Once the power and the speed for the ICE and the EM are set, calculate the torque for each.

The simulation results show a better performance of the strategy than a rule-based strategy based on ADVISOR. The results indicate that the ICE is, effectively, operated with high efficiency levels most of the time and that the speed and the power demanded by the driving cycles are accurately met. The results also demonstrate that this strategy is robust, from the driving cycle point of view, since it shows good performances for the UDDS driving cycle and the HWFET driving cycle for the same set of tuning parameters.

Ongoing and future work

There are several topics on this work which still need to be investigated:

(a) comparing the strategy with the DP solution as a way to evaluate its distance from the optimal performance;
(b) studying the effect on the performance of the strategy of using a priori information on the driving conditions;
(c) optimizing the size of the HEV power sources (the ICE, the EM and the battery) and the design of the manual transmission to improve the overall performance;
(d) testing the performance of the strategy with other controllers for the SOC compensator instead of the PI controller;
(e) testing the strategy on a real vehicle with the same powertrain configuration.

Investigations into all these points are ongoing.

Declaration of conflict of interest

The authors declare that there is no conflict of interest.

Funding

This work was supported by the Consejo Nacional de Ciencia y Tecnología (grant number 103640) and the Universidad Nacional Autónoma de México, Programa de Apoyo a Proyectos de Investigación e Innovación Tecnológica (grant number IN105512 and grant number IN 109414).

References

1. Gong Q, Li Y and Peng ZR. Trip-based optimal power management of plug-in hybrid electric vehicles. *IEEE Trans Veh Technol* 2008; 57(6): 3393–3401.
2. Schouten NJ, Salman MA and Kheir NA. Fuzzy logic control for parallel hybrid vehicles. *IEEE Trans Veh Technol* 2002; 10: 460–468.
3. Lin CC, Peng H, Grizzle JW and Kang JM. Power management strategy for a parallel hybrid electric truck. *IEEE Trans Control Systems Technol* 2003; 11(6): 839–849.
4. Musardo C, Rizzoni G and Staccia B. A-ECMS: an adaptive algorithm for hybrid electric vehicle energy management. In: *44th conference on decision and control and 2005 European control conference*, Seville, Spain, 12–15 December 2005, pp. 1816–823. New York: IEEE.
5. Sciarretta A, Back M and Guzzella L. Optimal control of parallel hybrid electric vehicles. *IEEE Trans Control Systems Technol* 2004; 12(3): 352–363.
6. Miller JM. Hybrid electric vehicle propulsion system architectures of the e-CVT Type. *IEEE Trans Power Electron* 2006; 21: 756–767.
7. Ehsani M, Gao Y and Miller JM. Hybrid electric vehicles: architecture and motor drives. *Proc IEEE* 2007; 95: 719–728.
8. Langari R and Won JS. Integrated drive cycle analysis for fuzzy logic based energy management in hybrid vehicles. In: *12th IEEE international conference on fuzzy systems*, St Louis, Missouri, USA, 25–28 May 2003, Vol 1, pp. 290–295. New York: IEEE.

9. Zhang C, Vahidi A, Pisu P et al. Role of terrain preview in energy management of hybrid electric vehicles. *IEEE Trans Veh Technol* 2010; 59(3): 1139–1147.
10. Lin CC, Peng H, Jeon S and Lee JM. Control of a hybrid electric truck based on driving pattern recognition. In: *6th advanced vehicle control conference*, Hiroshima, Japan, 9–13 September 2002, vol 42, pp. 41–58. Tokyo: JSAE.
11. Delprat S, Guerra TM, Paganelli G et al. Control strategy optimization for an hybrid parallel powertrain. In: *2001 American control conference*, Arlington, Virginia, USA, 25–27 June 2001, Vol 2, pp. 1315–1320. New York: IEEE.
12. Delprat S, Lauber J, Guerra TM and Rimaux J. Control af a parallel hybrid powertrain: optimal control. *IEEE Trans Veh Technol* 2004; 53(3): 872–881.
13. Kessels JTBA, Koot MWT, van den Bosch PPJ and Kok DB. Online energy management for hybrid electric vehicles. *IEEE Trans Veh Technol* 2008; 57(6): 3428–3440.
14. Paganelli G, Delprat S, Guerra TM et al. Equivalent consumption minimization strategy for parallel hybrid powertrains. In: *IEEE 55th vehicular technology conference*, Birmingham, Alabama, USA, 6–9 May 2002, Vol 4, pp. 2076–2081. New York: IEEE.
15. Borhan HA, Vahidi A, Phillips AM et al. Predictive energy management of a power-split hybrid electric vehicle. In: *2009 American control conference*, St Louis, Missouri, USA, 10–12 June 2009, pp. 3970–3976. New York: IEEE.
16. Johannesson L and Egardt B. Approximate dynamic programming applied to parallel hybrid powertrains. In: *17th IFAC world congress*, Seoul, Republic of Korea, 6–11 June 2008, p. 3374–3379. Laxenburg: IFAC.
17. van Keulen T, de Jager B, Serrarens A and Steinbuch M. Optimal energy management in hybrid electric trucks using route information. *Oil Gas Sci Technol* 2010; 65(1): 103–113.
18. Sciarretta A and Guzzella L. Control of hybrid electric vehicles. *Control Systems, IEEE* 2007; 27(2): 60–70.
19. Becerra G, Mendoza-Soto JL and Alvarez-Icaza L. Power flow control in hybrid electric vehicles. In: *ASME dynamic systems and control conference and Bath/ASME symposium on fluid power and motion control*, Arlington, Virginia, USA, 31 October–2 November 2011, Vol 2, paper DSCC2011-6062, pp. 255–262. New York: ASME.
20. Markel T, Brooker A, Hendricks T et al. ADVISOR: a systems analysis tool for advanced vehicle modeling. *J Power Sources* 2002; 110(2): 255–266.
21. Bellman R, Glicksburg I and Gross O. On the 'bang–bang' control problem. *Q Appl Math* 1956; 14: 11–18.
22. Gao DW, Mi C and Emadi A. Modeling and simulation of electric and hybrid vehicles. *Proc IEEE* 2007; 95(4): 729–745.
23. Schouten NJ, Salman MA and Kheir NA. Fuzzy logic control for parallel hybrid vehicles. *IEEE Trans Veh Technol* 2002; 10: 460–468.
24. National Renewable Energy Laboratory. ADVISOR Advanced Vehicle Simulator. http://adv-vehicle-sim.sourceforge.net/advisor_ch3.html#3.2 (2013, accessed 15 October 2014).

Appendix 1

Optimization of the speed of the internal-combustion engine

In this section an algorithm to find the most efficient ICE speed for a given power using an efficiency map is presented.

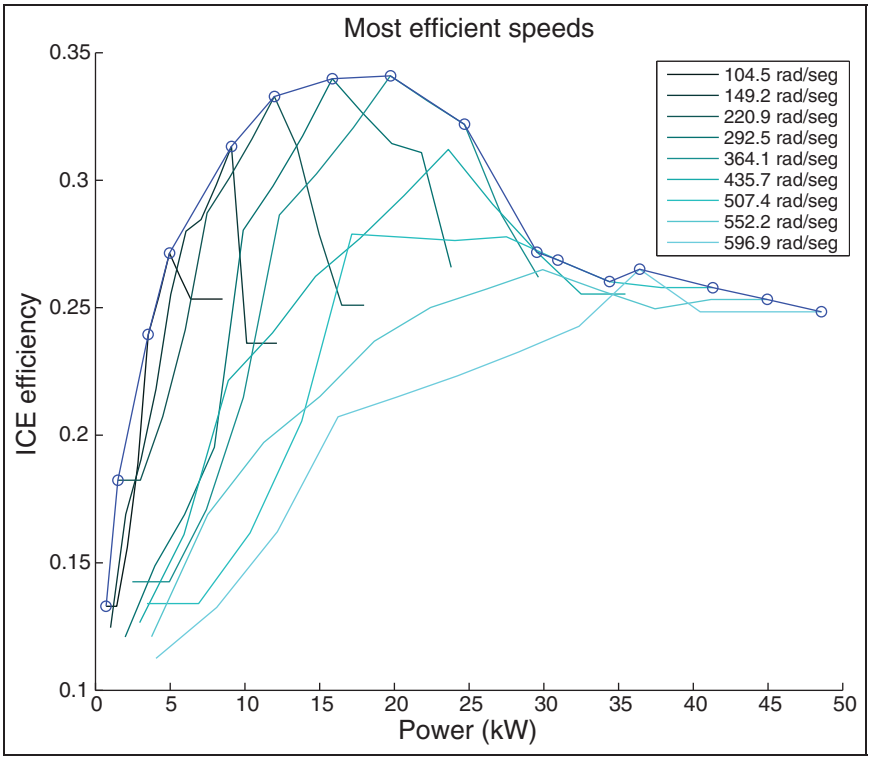

Figure 17. ICE power versus efficiency at constant speed.
ICE: internal-combustion engine.

Once $P_{ice}(t)$ has been set, it is necessary to determine the ICE speed $\omega_{ice}(t)$ in order to find the solution to equations (20) and (21). In the work by Becerra et al.,[19] $\omega_{ice}(t)$ is found using information given by the ICE manufacturer. This information is not always available; instead, efficiency maps presented as a table are used by most simulation tools.[20,22]

Given a table which maps $\omega_{ice}(t)$ and $\tau_{ice}(t)$ to an ICE efficiency $\mathrm{ICE}_{eff}(\omega_{ice}(t), \tau_{ice}(t))$ (i.e. an ICE efficiency map in table form), the following algorithm can be applied.

Step 1. Start with the lowest P_{ice} (and its corresponding minimum ω_{ice} and τ_{ice}) in the ICE efficiency map table, and take it as the base power P_{base} (and its corresponding ω_{base} and τ_{base}) for the first iteration.
Step 2. Search on the ICE efficiency map table for the largest neighbour to P_{base} (by increasing ω_{base} or τ_{base}) which offers the highest $\Delta\mathrm{ICE}_{eff}/\Delta P_{ice}$ with respect to P_{base}. The size of the search depends on the ICE and on the map, but it should be performed for neighbours within 10% of the maximum power.
Step 3. Add the power found in step 2, and its corresponding speed, to the table ω_{ice_eff}.
Step 4. Take as the new P_{base} the power found in step 2, and its corresponding ω_{base} and τ_{base}.
Step 5. Repeat from step 2 until the maximum power from the ICE efficiency map table is reached.
Step 6. The table generated in step 3 maps a given power to its most efficient speed; in other words, it generates $\omega_{ice\_eff}(P_{ice})(t)$.

Figure 17 shows the plot of $P_{ice}(t)$ versus $\mathrm{ICE}_{eff}(\omega_{ice}(t), \tau_{ice}(t))$ at a constant speed for the speeds defined in the ICE efficiency map table. The upper contour is the plot of the table $\omega_{ice\_eff}(P_{ice})(t)$ found with the previous algorithm for the ICE that was chosen for simulations in this work. The plot of $P_{ice}(t)$ versus $\omega_{ice\_eff}(P_{ice})(t)$ is shown in Figure 9.